AN APPROXIMATE MODEL FOR STUDYING HARMONIC CURRENT AMPLIFICATIONS IN CURRENT-SOURCE INVERTER FED INDUCTION MOTORS

Prepared by

J. S. Hsu

To be presented at the
IEEE Power Engineering Society 1992 Winter Meeting

July 1991

Publication No. PR-144
Center for Electromechanics
The University of Texas at Austin
Balcones Research Center
Blldg. 133, EME 1.100
Austin, TX 78758-4497
(512) 471-4496

AN APPROXIMATE MODEL FOR STUDYING HARMONIC CURRENT AMPLIFICATIONS IN CURRENT-SOURCE INVERTER FED INDUCTION MOTORS

John S. Hsu (Htsui)
Senior Member
Center for Electromechanics
The University of Texas at Austin
Austin, Texas 78712

Abstract: The nature of harmonic current amplification in the current-source inverter fed induction motors is studied through a six-pulse current-source inverter. An approximate model consisting of the induction motor and the parallel and series capacitors is used to simulate the circuit under the multiple commutation mode. The thyristor currents are treated as the source currents.

The analytical result shows that the steady phase harmonic current amplification of the six pulse inverter-fed motor goes from the high frequencies down to the fifth order of harmonic when the values of the capacitor reactances of the approximate model are reduced. Experimental study shows that the fifth harmonic current amplification is significant under a multiple commutation mode.

INTRODUCTION

The adjustable speed motors have undoubtedly gained their popularity. Generally speaking, the torques associated with the chopped supply of adjustable-speed drives inherently contain various contents of harmonics [1-6]. The torque pulsations affect the noise level and the smoothness of the torque of the drives. The natural frequencies of the mechanical system consisting of the motor and the driven equipment are intentionally diverted from the pulsating torque frequencies over the speed range of the adjustable-speed drive.

The six pulse, current-source inverter fed induction motor as shown in Fig. 1 is widely used. The inverter consists of six capacitors, six thyristors, and six diodes. The motor windings are part of the commutation circuit. The large dc link inductance is essential for maintaining a steady current source of the inverter. The dominant current harmonic orders are the fifth and the seventh. They cause significant sixth, twelfth, etc. torque pulsations [1] in the orders of the multiples of six.

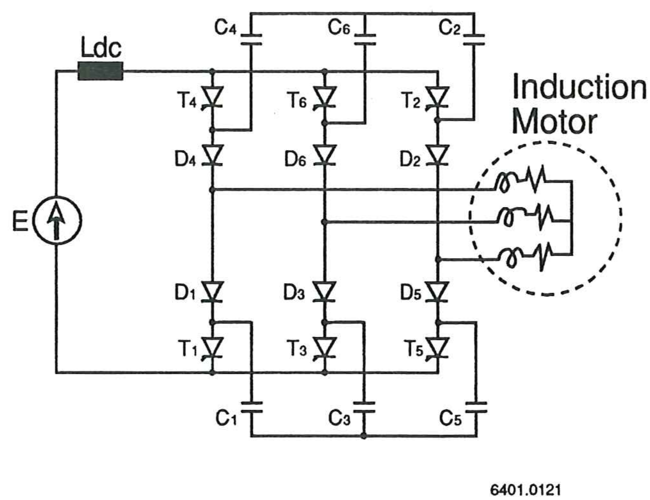

Fig. 1. Six pulse current source inverter fed induction motor

This type of current-source inverter fed drive is simple and can handle large power ratings with satisfactory performance. However, it is also known that in some occasions, when the natural frequencies of the mechanical systems were close to the frequencies of the excessive pulsating torques at certain speeds, damages to the couplings or to the shafts occurred. Since the excessive pulsating torques of a current-source inverter fed induction motor are produced by its excessive harmonic currents, a further understanding of the amplification of the harmonic currents is useful.

Lienau [2] observed that there are three commutation modes of the six-pulse current-source drive system; namely, the single, the double, and the multiple commutation modes. For the multiple commutation mode, Lienau points out that the circuit contains several energy storage devices, the diode current starts oscillating, the fifth harmonic of the motor currents are amplified. The analysis of this amplification from the motor, capacitors, and commutation standpoint is not included in Lienau's investigation.

With reference to the circuit shown in Fig. 1, several observations can be stated without going into detailed circuit analyses.

a) The combined currents of the motor and the capacitors, pass through the thyristors, the dc current source, and the dc-link inductor to complete the current paths.

b) The thyristors currents as shown in Fig. 2 are practically commutated instantaneously (in the order of tens of microseconds). Each rectangular wave represents 120° time span of the dc current. The thickened two rectangular waves represent the thyristors currents of a phase. The combined current of the three upper or lower thyristors of Fig. 1 goes through the large dc link inductor, L_{dc}, that suppresses the fluctuation. Consequently, the Fourier series of the thyristors phase current, for instance, i_{T4} and i_{T1} in Fig. 2 indicate that the phase harmonic currents riding on the fundamental current are mainly in the fifth and the seventh orders.

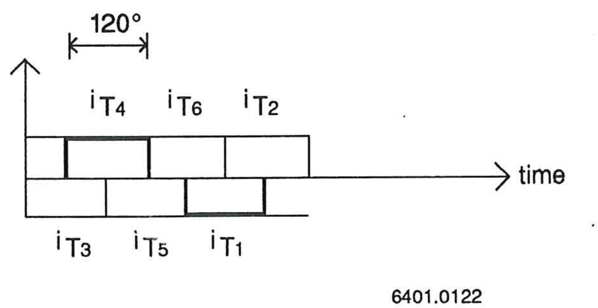

Fig. 2. Thyristor currents

c) The unidirectional nature of the thyristors and diodes dictates that when a harmonic current is going through a diode, the negative halves of the harmonic current must ride on the positive half of the fundamental current. The resultant current is fluctuating.

d) If the motor does not have any inductance and the turning-off of the thyristor does not require a forced commutation, there is no need to have capacitors. Under this hypothetical situation, the motor line current is the currents of the two thyristors connected to the same line.

e) However, in practice, the motor does have inductance and the thyristor requires a forced turnoff. The current in an inductor cannot be turned off instantaneously when the thyristor is turned off. The motor currents have to go through capacitors for dumping the magnetic energy associated with the currents. Here is where various commutation modes [2] take place affected by the motor, capacitors, the frequency, etc.

f) Under the single commutation mode [2], only three diodes in the inverter or a maximum of two diodes in one group (i.e. either the upper or the lower three diodes) are conducting during commutation.

g) Under the multiple commutation mode, the diode commutation takes a relatively longer time than that under the single commutation mode. There are diode commutations in both the upper and the lower groups simultaneously. The increased number of conducting diodes allow the harmonic currents to go directly between the motor terminals through the capacitors without going through the thyristors.

The corresponding circuit of the multiple commutation given by Lienau [2] is shown in Fig. 3. All the diodes and thyristors shown in this figure are conducting. The thyristor current, i_{T4}, goes through a parallel capacitor path corresponding to the circuit branch with D_3, D_6, and two capacitors. The thyristor current also goes through series capacitors and motor windings corresponding to the phases with D_1 and D_2.

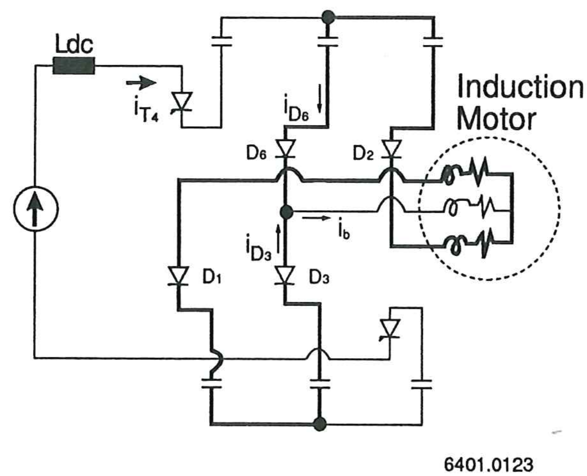

Fig. 3. Circuit under multiple commutation mode -- all diodes and thyristors shown here are conducting

ASSUMPTIONS

The analysis is based on the following assumptions:

a) During the multiple commutation mode, the effective circuit for the analysis is shown in Fig. 4. It is assumed that this circuit consisting of the equivalent parallel capacitors, C, and the series capacitors, Cs, that are connected in series with the windings. The thyristors currents referring to each phase are the current sources of this three-phase analytical model. The approximation comes from using a symmetrical circuit (Fig. 4) to roughly represent an asymmetrical circuit (Fig. 3). This approximation is justified for the initial investigation of the harmonic current amplification without excessive analysis.

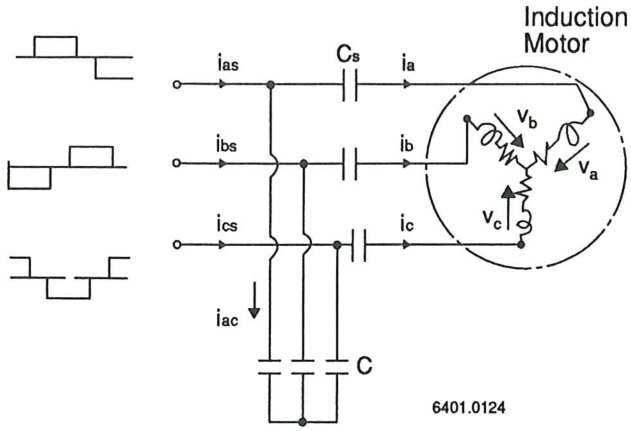

Fig. 4. Effective circuit of the analytical model

b) The per-unit values of the parallel and series capacitor reactances X_c and X_{cs} are assumed to be the same as the lower or upper per phase commutation capacitor.

c) The inductance of the dc link is sufficiently high and the commutation time of the thyristors is negligible to assume the rectangular shape of the thyristors currents.

d) The motor runs at a constant speed. Experimental result shows that even at low frequency (5 Hz) [1], with a small pulsation of the speed the performance calculation under this assumption is still acceptable.

e) Saturated motor parameters are used, otherwise the motor magnetic circuit is considered to be linear.

f) Core, friction, windage, and stray-load losses are not considered in the analysis.

g) The neutral of the motor is not grounded; consequently, the current and flux linkage of coordinate zero can be neglected. It is worth mentioning that the current and flux of coordinate zero, even if they exist, do not produce torque.

ANALYSIS

There are different coordinate systems that can be used for analyses [7-14]. This paper uses the 1-2-0 coordinate system [9,14] and the per unit values for the analysis. Since the value of coordinate 2 is always the conjugate complex number of the value of coordinate 1, attention can be drawn mainly to the values referring to coordinate 1. Resultant equations established in the available literature, such as the transformation from a, b, c values to 1, 2, 0 values, or vice versa [9,14], and the definition of the operational impedances [14] are mentioned and used directly without repeating the derivations.

The input data, the unit (or base) values, the basic conversions between a, b, c and 1, 2, 0 coordinates, and the source currents are given in Appendices 1, 2, 3, and 4, respectively.

The chopped source currents, i_{as}, i_{bs}, and i_{cs}, of the analytical model shown in Fig. 5a can be transformed to the 1-2-0 coordinate values shown in Fig. 5b through the equations for coordinate conversions given in Appendix 3. The real and imaginary parts of the coordinate-1 current i_{1s} of the source currents are shown in Fig. 5b.

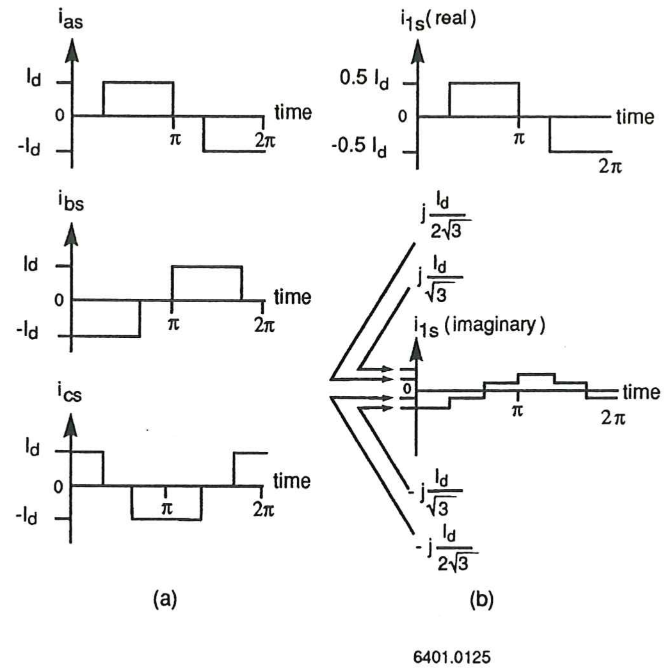

Fig. 5. Three-phase source currents:
a) i_{as}, i_{bs}, and i_{cs}
b) real and imaginary parts of i_{1s}

The coordinate-1 value, i_{1s}, of the source current contains the motor current i_{1m} that goes through the series capacitor and the motor phase winding, and the parallel capacitor current i_{1c}. These currents refer to the motor and parallel capacitor currents shown in Fig. 4.

$$L\, i_{1S} = L\, i_{1m} + L\, i_{1c} = \left[\frac{1}{R_S + P\,X(P-j\omega) + \frac{X_{CS}}{P}} + \frac{1}{X_C}P\right] L\, v_{1S} \quad (1)$$

where the symbol L stands for the P-multiplied Laplace transform. P is a parameter used for the Laplace transform. When applying the Laplace transform to solve a differential equation, P also stands for d/dt of a function while the initial value of the function is 0. The operational impedance $X(P-j\omega)$ of the induction motor is given in Appendix 5.

Motor Currents

The motor current, i_{1m}, of coordinate 1 is the same as the series capacitor current. It can be calculated through

$$L\, i_{1m} = \frac{L\, v_{1S}}{R_S + P\,X(P - j\omega) + \frac{X_{CS}}{P}}$$

Substituting $L v_{1S}$ from (1)

$$L\, v_{1S} = \frac{L\, i_{1S}}{\left[\frac{1}{R_S + P\,X(P - j\omega) + \frac{X_{CS}}{P}} + \frac{1}{X_C} P\right]}$$

into the above equation gives

$$L\, i_{1m} = \frac{X_C\, L\, i_{1S}}{\left[X_C + \left[R_S + P\,X(P - j\omega) + \frac{X_{CS}}{P}\right] P\right]} \qquad (2)$$

Substituting $L\, i_{1S}$ and $X(P - j\omega)$ given in Appendices 4 and 5 into the above equation, $L\, i_{1m}$ becomes

$$L\, i_{1m} = \frac{N(P)\left(P - j\,\omega + \frac{1}{T_2}\right) I_d}{\left\{ D_2(P)\, 2\cosh\left(\frac{\pi}{2} P\right) \right\}} \qquad (3)$$

where

$$N(P) = X_C \left\{ \begin{array}{l} \left(0.5\, e^{(\pi/6)P} - 0.5\, e^{-(\pi/2)P}\right) \\ + j\left(-\frac{1}{\sqrt{3}} e^{(\pi/2)P} + \frac{1}{2\sqrt{3}} e^{(\pi/6)P}\right) \left(1 - e^{-(2\pi/3)P}\right) \end{array} \right\}$$

$$D_2(P) = P^3 A_1 + P^2 A_2 + P A_3 + A_4$$

and

$$A_1 = X_{ss}\tau$$

$$A_2 = \frac{X_{ss}}{T_2} - X_{ss}\, j\,\omega\tau + R_S$$

$$A_3 = \frac{R_S}{T_2} + X_C + X_{CS} - R_S\, j\,\omega$$

$$A_4 = \frac{X_C}{T_2} - X_C\, j\,\omega - X_{CS}\, j\,\omega + \frac{X_{CS}}{T_2}$$

The inverse Laplace transform of $L\, i_{1m}$ of (3) can be solved using the residue theorem [15, 16] or the Heaviside expansion formula [15]. Any appropriate method, such as the Newton-Raphson method, can be used to solve the values of the roots of the denominator of (3). There are three roots, P_Q, where Q=1, 2, and 3, of the denominator term

$$D_2(P) = 0$$

and a series of roots $P_{(k)}$ solved from the other denominator term

$$\cosh(\pi P/2) = 0.$$

where

$$P_{(k)} = (2k + 1)\, j$$

and $k = 0, \pm 1, \pm 2 \ldots$

The inverse Laplace transform of $L\, i_{1m}$ obtained through Heaviside expansion formula can be written as

$$i_{1m} = \sum_{Q=1}^{Q=3} \frac{N(P)\left(P - j\,\omega + \frac{1}{T_2}\right) I_d\, e^{P_Q t}}{P_Q \left.\frac{d\left[2 D_2(P) \cosh\left(\frac{\pi}{2} P\right)\right]}{dP}\right|_{P_Q}} + \sum_{k=-\infty}^{k=+\infty} \frac{N(P)\left(P - j\,\omega + \frac{1}{T_2}\right) I_d\, e^{P_{(k)} t}}{P_{(k)} \left.\frac{d\left[2 D_2(P) \cosh\left(\frac{\pi}{2} P\right)\right]}{dP}\right|_{P_{(k)}}}$$

Since

$$\frac{d\left[2 D_2(P) \cosh\left(\frac{\pi}{2} P\right)\right]}{dP} = 2 D_2'(P) \cosh\left(\frac{\pi}{2} P\right) + \pi\, D_2(P) \sinh\left(\frac{\pi}{2} P\right)$$

where

$$D_2'(P) = 3A_1 P^2 + 2 A_2 P + A_3$$

Considering

$$\cosh\left(\frac{\pi}{2} P_{(k)}\right) = \cosh\left[\frac{\pi}{2}(2k + 1)\, j\right] = \cos\left[\frac{\pi}{2}(2k + 1)\right] = 0$$

$$D_2(P_Q) = 0$$

and

$$\sinh\left(\frac{\pi}{2} P_{(k)}\right) = j \sin\left[\frac{\pi}{2}(2k + 1)\right] = j\,(-1)^k$$

the motor current i_{1m} of coordinate 1 becomes

$$i_{1m} = \sum_{Q=1}^{Q=3} \frac{N(P_Q)\left(P_Q - j\,\omega + \frac{1}{T_2}\right) I_d\, e^{P_Q t}}{P_Q\left[2 D_2'(P_Q) \cosh\left(\frac{\pi}{2} P_Q\right)\right]} + \sum_{k=-\infty}^{k=+\infty} \frac{N(P_{(k)})\left(P_{(k)} - j\,\omega + \frac{1}{T_2}\right) I_d\, e^{P_{(k)} t}}{P_{(k)}\left[\pi\, D_2(P_{(k)})\, j\,(-1)^k\right]} \qquad (4)$$

The phase-a motor current, i_a, is

$$i_a = i_{1m} + i_{2m} \qquad (5)$$

where i_{2m} is the conjugated value of i_{1m} and i_{0m} is assumed to be zero.

Motor Phase Voltage

According to the definition [14], the motor phase voltage of coordinate 1 can be represented as

$$v_{1m} = L^{-1}\left[P\left(L\, \psi_{1m}\right)\right] + R_S\, i_{1m} \qquad (6)$$

where the P-multiplied Laplace transform of the derivative of the flux linkage, $P\left(L\, \psi_{1m}\right)$, is the product of P, the operational impedance at speed ω, and the current.

$$P\left(L\, \psi_{1m}\right) = P\, X(P - j\,\omega)\, L\, i_{1m}$$

Substituting $X(P - j\,\omega)$ and $L\, i_{1m}$ from Appendix 5 and equation (3) into the above equation gives

$$L^{-1}\left[P\left(L\, \psi_{1m}\right)\right] = \frac{d\, \psi_{1m}}{d\,t} = L^{-1}\left\{ \frac{P\, X_{ss}\left[\tau\,(P - j\,\omega) + \frac{1}{T_2}\right] N(P)\, I_d}{2 D_2(P) \cosh\left(\frac{\pi}{2} P\right)} \right\}$$

The inverse Laplace transform can be solved using the same manner as that for the solution of the motor current. The coordinate-1 motor phase voltage of (6) can be obtained from

$$v_{1m} = R_S\, i_{1m} + \sum_{Q=1}^{Q=3} \frac{P_Q X_{ss}\left[\tau\,(P_Q - j\,\omega) + \frac{1}{T_2}\right] N(P_Q)\, I_d\, e^{P_Q t}}{P_Q\left[2 D_2'(P_Q) \cosh\left(\frac{\pi}{2} P_Q\right)\right]} + \sum_{k=-\infty}^{k=+\infty} \frac{P_{(k)} X_{ss}\left[\tau\,(P_{(k)} - j\,\omega) + \frac{1}{T_2}\right] N(P_{(k)})\, I_d\, e^{P_{(k)} t}}{P_{(k)}\left[\pi\, D_2(P_{(k)})\, j\,(-1)^k\right]} \qquad (7)$$

The phase-a voltage v_a is

$$v_a = 2\ \mathrm{Real}\,(v_{1m}) \tag{8}$$

where $v_{0m} = 0$.

SAMPLE CALCULATION OF THE MODEL

The condition for applying this model is that the multiple commutation mode has taken place. The parameters of a 3-phase, 4-pole, Y-connected squirrel-cage motor are derived from the 60-Hz values and given as follows:

frequency (Hz)	=	60	30
unit torque (Nm)	=	19.79	39.58
unit current (A)	=	9.36	9.36
unit voltage (V)	=	132.79	132.79
unit impedance (Ω)	=	14.18	14.18
Xls (p.u.)	=	0.0628	0.0314
Xlr (p.u.)	=	0.0628	0.0314
Xm (p.u.)	=	1.7630	0.8814
Rs (p.u.)	=	0.0395	0.0395
Rr (p.u.)	=	0.0240	0.0240
Id (p.u.)	=		1.0
N (r/min)	=		886.

A series of computations for obtaining the motor currents and voltages through (5) and (8) are conducted with various values of capacitor reactances, X_c and X_{cs}, at 30 Hz. When there is no parallel capacitor connected to the motor, the X_c value is infinity, a large value of $X_c = 1{,}000$ is used to represent this situation. The steady-state value is obtained by starting the computation of the current at 200 cycles to allow the attenuation of the initial transients.

Fig. 6 shows the motor phase-a, steady-state, per-unit current and voltage. When there is no capacitor ($X_c = 1{,}000$, and $X_{cs} = 0$) connected to the motor, the motor currents calculated from the model are in rectangular shapes. This is close to the situation when the inverter is under single commutation mode. The spikes of the motor voltage correspond to the steps of the current source.

Fig. 7 shows that the higher frequency harmonic currents of the motor are amplified when the capacitances are small (i.e. X_c and X_{cs} are large). The overall magnitudes of both the current and voltage are low as compared with those under the single commutation mode given in Fig. 6.

Fig. 8 shows that the seventh-harmonic current amplification occurs while certain amounts of capacitances are connected to the motor as indicated by the current and voltage waveforms at $X_c = 1.5$ and $X_{cs} = 1.5$.

Fig. 9 shows that when more capacitances are connected to the motor, the fifth harmonic current amplification becomes significant. This is represented by the motor current and voltage waveforms of $X_c = 0.8$

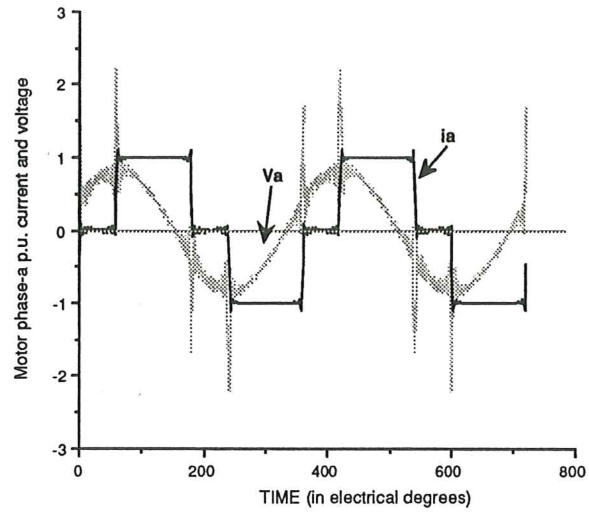

6401.0126

Fig. 6. Motor phase-a per unit current and voltage without capacitors at 30 Hz

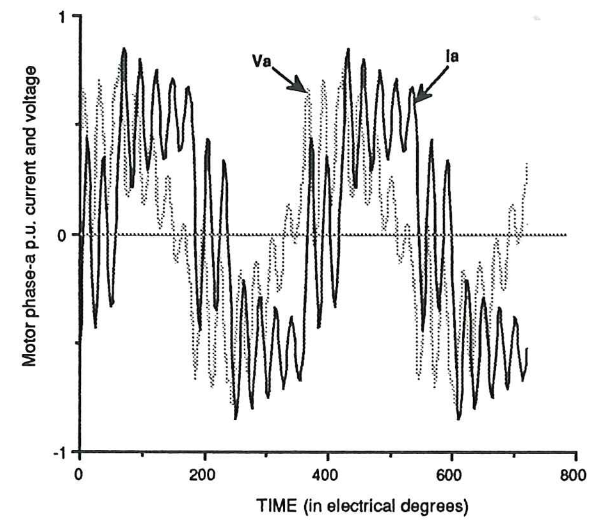

6401.0127

Fig. 7. Motor phase-a per unit current and voltage with $X_c = 6$ and $X_{cs} = 6$ at 30 Hz

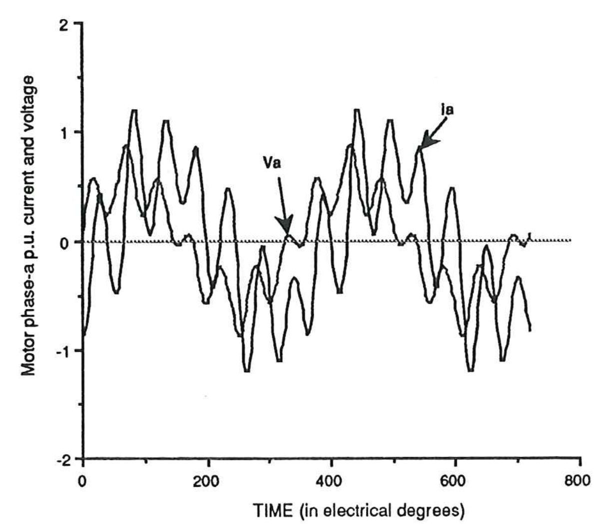

6401.0128

Fig. 8. Motor phase-a per unit current and voltage with $X_c = 1.5$ and $X_{cs} = 1.5$ at 30 Hz

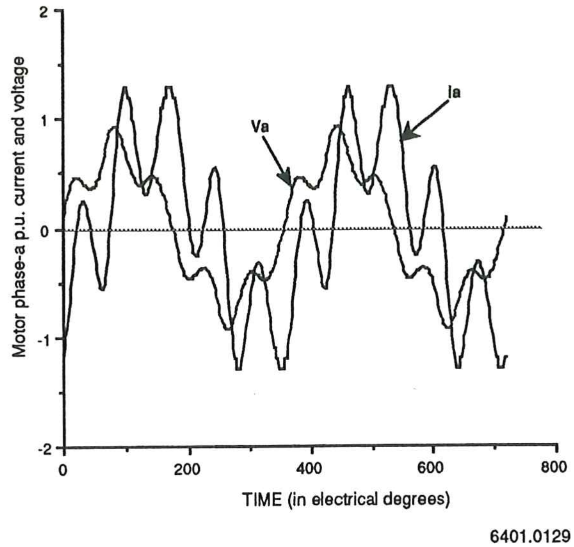

Fig. 9. Motor phase-a per unit current and voltage with $X_c = 0.8$ and $X_{cs} = 0.8$ at 30 Hz

and $X_{cs} = 0.8$. The fundamental component of the voltage corresponding to a 1.0 per-unit source current is lower than that shown in Fig. 6 under the single commutation mode.

If the capacitances connected to the motor keep increasing, analytical results show that a normal motor operation cannot be sustained under this situation.

COMPARISON BETWEEN EXPERIMENTAL OBSERVATIONS AND ANALYTICAL RESULTS

Figs. 10, 11, and 12 show the diode currents i_{D3}, i_{D6}, the motor current i_b, and the line voltage v_{line}, tested at 34, 40, and 46.5 Hz, respectively. The summation of the diode currents i_{D3} and i_{D6} is the motor phase current i_b. The discrepancies in shapes between the summation of the diode currents and the motor phase current i_b are caused by two reasons: 1) The use of different types of current shunts. The resistance current shunts are used for the measurement of the diode currents, and a Hall-effect isolated current shunt is used for the measurement of i_b. 2) The time instant for sampling the data for the upper two traces is different from that for the lower two traces in the experimental traces shown in Figs. 10, 11, and 12. This time difference is caused by a digital acquisition equipment.

Totally, six 34-μF capacitors are connected in two deltas for the upper and lower commutation capacitors shown in Fig.1. Three 8.8 mH per phase inductors are connected in series with the motor to create a multiple commutation mode. This mode that starts at 46.5 Hz is judged by the occurrence of the simultaneous conductions of the diode currents i_{D3} and i_{D6} shown in Fig. 12. A significant fifth harmonic component is shown in the phase current i_b while a multiple commutation mode is taking place.

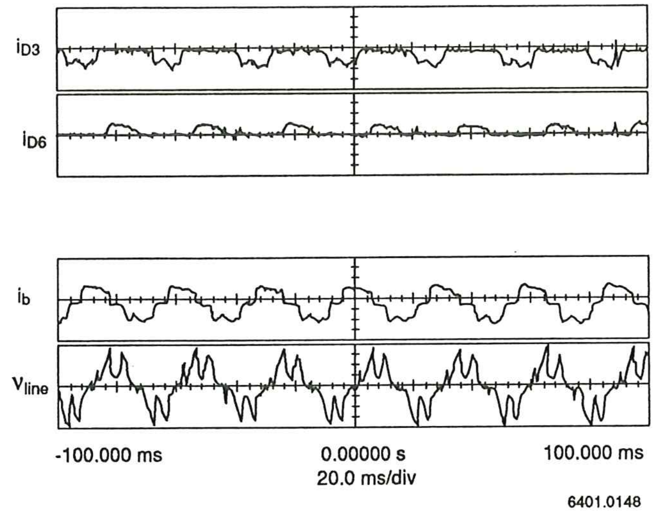

Fig. 10. Tested current and line voltage at 34 Hz

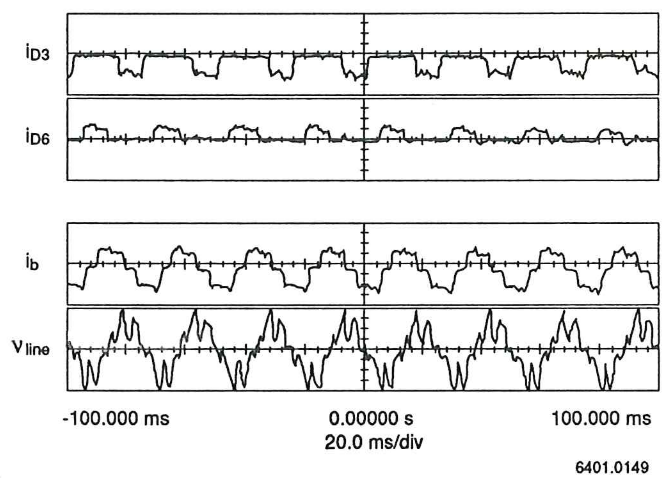

Fig. 11. Tested current and line voltage at 40 Hz

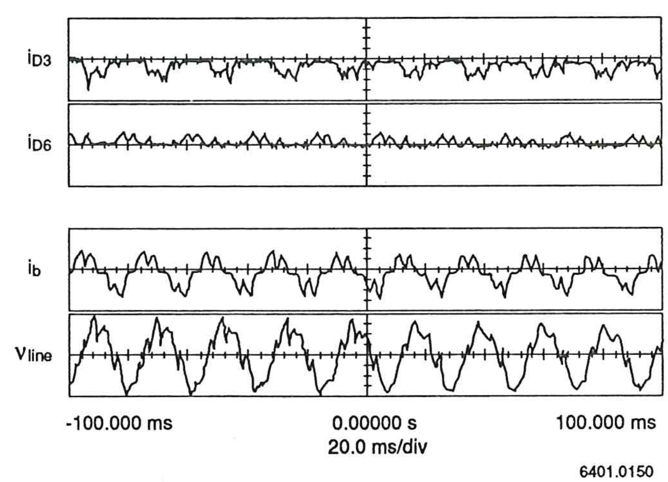

Fig. 12. Tested current and line voltage at 46.5 Hz

The corresponding calculated current i_b with the parameters of the test setup at 46.5 Hz is shown in Fig. 13. A fifth harmonic component can be identified easily from the current waveform. The parameters in per unit (p.u.) values used in this calculation are:

X_c	= 2.4	X_{cs}	= 2.4
X_{ls}	= 0.2300	X_{lr}	= 0.0487
X_m	= 1.3663	R_s	= 0.0395
R_r	= 0.0240	N	= 1,380 rpm
p	= 4		

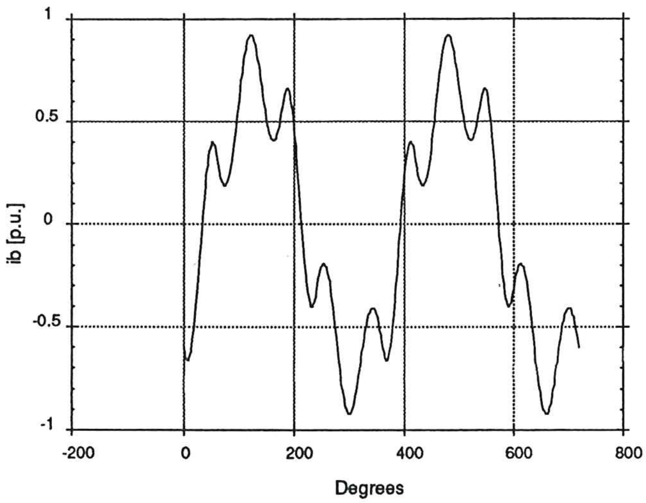

6401.0162

Fig. 13. Calculated current i_b at 46.5 Hz

CONCLUSION

The torques associated with the chopped supplies of adjustable-speed drives inherently contain various contents of harmonics. The torque pulsations affect the noise level and the smoothness of the torque of the drives.

The current-source inverter fed drive is simple and can handle large power ratings with satisfactory performance. However, it is also known that it is possible to have excessive pulsating torques that are related to the excessive harmonic currents of the motor. In order to avoid an over-complex analysis for the asymmetrical circuit under a multiple commutation mode, an approximate symmetrical model is used for studying the nature of harmonic current amplification in current-source inverter fed induction motors.

A series of computations is conducted to identify the harmonic-current amplifications with various capacitor values under a multiple commutation mode. The harmonic current amplification goes from the high frequencies down to the fifth harmonics, when the value of the capacitor reactance reduces.

The experimental result of the harmonic current amplification is approximately in shape with the calculated result. The fifth harmonic currents are the major harmonic components in both the tested and the calculated currents.

ACKNOWLEDGEMENT

The author would like to thank the State of Texas for financial support through a grant under Texas Advanced Technology Program, Grants No. 1591 and No. 003658-181. This work has been partially supported by NSF Grant No. ECS-880884, which is gratefully acknowledged. Thanks are due to the Center for Electromechanics, The University of Texas at Austin, for the support staff and facilities provided for the research work. Finally, the author would like to express his deep appreciation to Dr. Herbert Woodson and Prof. W. Weldon for their leadership in this research.

REFERENCES

[1] Hsu, J. S., Amin, A. M. A., "Torque Calculations of Current Source Induction Machines Using the 1-2-0 Coordinate System," *IEEE Transactions on Industrial Electronics,* Vol. 37, No. 1, February, 1990, pp. 34-40.

[2] Lienau, W.,"Commutation Modes of A Current-Source Inverter," Proc. of 2nd IFAC Symposium on Control in Power Electronics and Electrical Drives, Pergamon Press, 1977, pp. 219-229.

[3] Novotny, D. W., "Steady State Performance of Inverter Fed Induction Machines by Means of Time Domain Complex Variables," *IEEE Transactions on Power Apparatus and Systems,* Vol. PAS-95, No. 3, May/June, 1976, pp. 927-935.

[4] Palmquist, Roland E., Guide to The 1971 National Electrical Code, Howard W. Sames & Co., Inc., Indianapolis, Indiana, 1972.

[5] Lipo, T. A., "Analysis and Control of Torque Pulsations in Current Fed Induction Motor Drives," IEEE 1978 Power Elec. Spec. Conf., 1978, pp.89-96.

[6] Bowes, S. R., Bullough, R. I., "Optimal PWM Microprocessor-Controlled Current-Source Inverter Drives," IEE Proceedings, Vol. 135, Pt. B, No. 2, March, 1988, pp. 59-75.

[7] Park, R. H., "Two-Reaction Theory of Synchronous Machines," *AIEE Transactions,* Vol. 48, p. 718.

[8] Stanley, H. C., "An Analysis of The Induction Machines," *AIEE Transactions,* Vol. 57, p. 751.

[9] Lyon, W. V., Transient Analysis of Alternating Current Machinery, An Application of The Method of Symmetrical Components, Wiley, 1954.

[10] Rankin, A. W., "Asynchronous and Single-Phase Operation of Synchronous Machines," *AIEE Transactions*, 1945.

[11] Htsui, J. S. C., "Non-Simultaneous Reclosing Air-Gap Transient Torque of Induction Motor: Part I, Analysis and Computation Logic," *IEEE Transactions on Energy Conversion,* Vol. EC-2, No. 2, June 1987, pp. 269-275.

[12] Htsui, J. S. C., "Non-Simultaneous Reclosing Air-Gap Transient Torque of Induction Motor: Part II, Sample Studies and Discussion on Reclosing of ANSI C50.41," *IEEE Transactions on Energy Conversion*, Vol. EC-2, No. 2, June 1987, pp.276-284.

[13] Htsui, J. S. C., "Magnitude, Amplitudes and Frequencies of Induction Motor Air-Gap Transient Torque Through Simultaneous Reclosing with or without Capacitors," *IEEE Transactions on Power Apparatus and Systems,* Vol. PAS-104, No.6, pp.1519-26, June, 1985.

[14] Kao, Jing-Tak, Analyses of Transients and Operating Conditions of Alternating Current Machinery, (Published in Chinese), Second Edition, Beijing, China: Science Press, 1962, pp. 55-102 and pp. 441-487.

[15] Pipes, Louis A., Applied Mathematics for Engineers and Physicists, second edition. New York: McGraw-Hill Book Company, Inc., 1958.

[16] Spiegel, Murray R., Theory and Problems of Laplace Transforms, Schaum's Outline Series, McGraw-Hill Book Company, New York, 1965.

[17] Htsui, J. S. C., Shepherd, W., "Method of Digital Computation of Thyristor Switching Circuits," *Proc. IEE,* Vol. 118, No. 8, August 1971, pp. 993-998.

APPENDIX 1
Input Data

The symbols of the input data are chosen as follows:

p	number of poles
f	line frequency (Hz)
X_{ls}	stator leakage reactance (per unit value)
X_{lr}	rotor leakage reactance (per unit value)
R_s	stator resistance (per unit value)
R_r	rotor resistance (per unit value)
X_m	magnetizing reactance (per unit value)
X_C	reactance of parallel capacitors C (per unit value)
X_S	reactance of series capacitors C_s (per unit value)
I_d	dc current (per unit value)
N	shaft speed (r/min)

APPENDIX 2
Base Values

The unit (or base) value of time is ($1/2\pi f$). As far as the equations in this paper are concerned there is no restriction for selecting the unit values based on either the input or the output of the electrical machine. However, since the calculation is mainly for motors, the shaft output is chosen as the unit power for convenience. The unit values under a particular frequency can be defined as follows:

Unit power [W]	746 • hp = motor output power
Unit voltage [V] =	phase voltage
Unit current [A] =	unit power/(No. of phases • unit voltage]
Unit impedance [Ω]	unit voltage/unit current
Unit torque [Nm]	unit power • (p/2)/(2πf)

APPENDIX 3
Coordinate Conversions

The following equations can be used for the coordinate conversions between the a-b-c and 1-2-0 systems.

$$i_1 = \frac{1}{3}\left(i_a + a\,i_b + a^2 i_c\right) \qquad i_a = i_1 + i_2 + i_0$$

$$i_2 = \frac{1}{3}\left(i_a + a^2 i_b + a\,i_c\right) \quad \text{or} \quad i_b = a^2 i_1 + a\,i_2 + i_0$$

$$i_0 = \frac{1}{3}\left(i_a + i_b + i_c\right) \qquad i_c = a\,i_1 + a^2 i_2 + i_0$$

where $a = e^{\frac{j2\pi}{3}} = -0.5 + j\,0.866$

APPENDIX 4
Source Currents

The value of the coordinate-1 source current i_{1s} changes at every $\pi/3$ radians. Using Heaviside unit functions, i_{1s} can be expressed as

$$i_{1S} = \left(0 - j\frac{I_d}{\sqrt{3}}\right)u(t-0) + \left(\frac{I_d}{2} + j\frac{I_d}{2\sqrt{3}}\right)u\left(t-\frac{\pi}{3}\right)$$
$$+ \left(0 + j\frac{I_d}{\sqrt{3}}\right)u\left(t - \frac{2\pi}{3}\right) + \left(-\frac{I_d}{2} + j\frac{I_d}{2\sqrt{3}}\right)u(t-\pi)$$

+ repeats in like manner in opposite direction over every π, up to time t

where the Heaviside unit function is defined through an example:

$$u\left(t-\frac{\pi}{3}\right) \qquad \begin{cases} u\left(t-\frac{\pi}{3}\right) = 1 & t > \frac{\pi}{3} \\ u\left(t-\frac{\pi}{3}\right) = 0 & t < \frac{\pi}{3} \end{cases}$$

The P-multiplied Laplace transform [15] is used in this study. Using L to represent this transform, the current i_1 can be written according to the definition of the P-multiplied Laplace transform.

$$L\; i_{1S} = P\int_0^\infty i_{1S}\, e^{-Pt}\, dt$$
$$= \frac{\left(0.5\, e^{(\pi/6)P} - 0.5\, e^{-(\pi/2)P}\right)}{2\cosh\left(\frac{\pi}{2}P\right)} I_d$$
$$+ j\frac{\left(-\frac{1}{\sqrt{3}}e^{(\pi/2)P} + \frac{1}{2\sqrt{3}}e^{(\pi/6)P}\right)\left(1 - e^{-(2\pi/3)P}\right)}{2\cosh\left(\frac{\pi}{2}P\right)} I_d$$

APPENDIX 5
Motor Operational Impedance

The operational impedance $X(P-j\omega)$ of the induction motor from [14] at a constant speed, ω, is

$$X(P-j\omega) = \frac{X_{ss}\left[\tau(P - j\omega) + \frac{1}{T_2}\right]}{P - j\omega + \frac{1}{T_2}}$$

and

$$\omega = \frac{\pi N p}{60\,\omega_s} \qquad \tau = 1 - \frac{X_m^2}{X_{ss} X_{rr}}$$

$$X_{ss} = X_{ls} + X_m \qquad \omega_s = 2\pi f$$

$$T_2 = \frac{X_{rr}}{R_r} \qquad X_{rr} = X_{lr} + X_m$$

John S. Hsu (or Htsui) (M '64, SM '90) was born in China. He received a BS degree from Tsing-Hua University, Beijing, China, and a PhD degree from Bristol University, England, in 1959 and 1969, respectively. He joined the Electrical and Electronics Engineering Department of Bradford University, England, serving there for nearly two years.

After his arrival in the United States in 1971, he worked in research and development areas for Emerson Electric Company and later for Westinghouse Electric Corporation. he served as head of the Rotating Machines and Power Electronics Program, Center for Energy Studies, The University of Texas at Austin for over four years. Presently, he is the manager of the Industrial Drive Program at the Center for Electromechanics at The University of Texas at Austin.

Dr. Hsu is a chartered engineer in the United Kingdom and a registered professional engineer in Texas, Missouri, and New York.